Review
Self-propagating high-temperature (combustion) synthesis (SHS) of powder-compacted materials

H. C. YI
Department of Chemical and Materials Engineering, University of Auckland, Auckland, New Zealand

J. J. MOORE
Department of Metallurgical and Materials Engineering, Colorado School of Mines, Golden, Colorado 80401, USA

Self-propagating high-temperature synthesis (SHS) of powder compacts is a novel processing technique currently being developed as a route for the production of engineering ceramics and other advanced materials. The process, which is also referred to as combustion synthesis, provides energy- and cost-saving advantages over the more conventional processing routes for these materials. At the same time, the rapid heating and cooling rates provide a potential for the production of metastable materials with new and, perhaps, unique properties. This paper reviews the research that has been, and is being, undertaken in this exciting new processing route for high-technology materials and examines the underlying theoretical explanations which will, eventually, lead to improved control over processing parameters and product quality.

1. Introduction

The conventional production of high-temperature refractory materials incurs costly penalties in both energy and time, because both high-temperature furnaces and long processing times are required. Recently, a novel processing technique, termed self-propagating high-temperature synthesis (SHS) or combustion synthesis has been used to synthesize refractory materials such as ceramics, ceramic composites and intermetallic compounds [1, 2]. This technique is concerned with the ignition of a compressed powder mixture, in either air or an inert atmosphere, producing a chemical reaction, with sufficient heat release (exothermic reaction) that it becomes self-sustaining.

There are two basic modes of combustion reactions: "propagating" and "bulk" reactions. A propagation reaction occurs when the powder reactants are ignited locally followed by a synthesis (combustion) wave passing through the compact. Bulk reactions occur when the powder compact is heated rapidly (e.g. in a furnace) until the synthesis reaction occurs simultaneously through the whole sample. This is also called a "thermal explosion". During the process the maximum or combustion temperature (T_c) reaches a very high level (e.g. $> 2000°$ C).

Researchers in the Soviet Union have lead the way in this research area. Originally started in the late 1960s, the Russians have now produced more than 500 materials using the SHS method, including electronic materials, metallic and ceramic superconductors, composites, intermetallics, refractories, abrasives and lubricants. Some of these are in commercial production. Recently, considerable interest in SHS has been generated in the USA and Japan. Several research institutes and universities in the USA are involved and have now successfully synthesized nitrides, borides, carbides, ceramic composites and some intermetallic compounds. Using densification methods it has been possible to produce high-density materials.

Some advantages have been reported for advanced materials produced by combustion synthesis. Because the extremely high temperatures vaporize volatile contaminants, the products are usually of a high purity [3]. Owing to the high cooling rates, high defect concentrations and non-equilibrium structures exist in the SHS-produced materials resulting in more reactive, metastable products. This has produced materials which are more sinterable [4], although some work has shown that the higher sintering activity [5] occurs only in the initial sintering period.

Also, because high-temperature furnaces are not required and the processing times are of the order of seconds instead of hours or days, as with normal sintering, savings with respect to energy and time can be made.

Some of the main SHS materials produced are listed in Table I, together with some of their combustion temperatures.
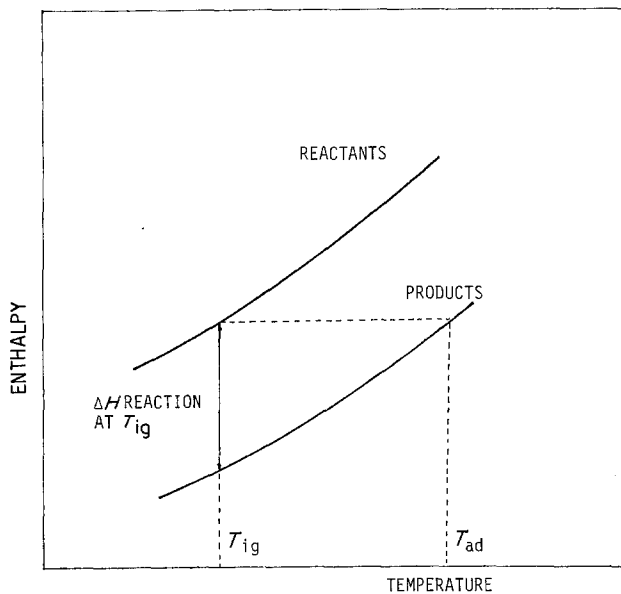
Figure 1 Diagrammatic representation of the calculation of the adiabatic temperature (T_{ad}).

2. Combustion theory and observations
2.1. Thermodynamic considerations
Once ignited, extremely high temperatures can be achieved in very short times, e.g. 2 to 3 sec, due to the highly exothermic nature of the reactions. It is therefore reasonable to assume that a thermally isolated exothermic system exists because there is very little time for the heat to disperse to its surroundings. Therefore, the maximum temperature to which the product is raised can be assumed to be the adiabatic temperature, T_{ad} [6, 7].

As the enthalpy of the system is a state function, the

TABLE I SHS produced materials and their combustion temperatures (K)

Borides	TiB$_2$ (3190), ZrB$_2$ (3310), NbB$_2$ (2400), TaB$_2$ (3370), MoB$_2$ (1800), LaB$_6$ (2800), HfB$_2$, CrB, VB.
Carbides	TiC (3210), HfC (3900), B$_4$C (1000), Al$_4$C$_3$ (1200), TaC (2700), SiC (1800), WC (1000), ZrC (3400), NbC (2800), Cr$_3$C$_2$.
Carbonitrides	TiC–TiN, NbC–NbN, TaC–TaN.
Nitrides	TiN (4900), ZrN (4900), BN (3700), AlN (2900), Si$_3$N$_4$ (4300), TaN (3360), HfN (5100), NbN.
Silicides	MoSi$_2$ (1900), Ti$_5$Si$_3$ (2900), Zr$_5$Si$_3$ (2800), Nb$_5$Si$_3$ (3340) NbSi$_2$ (1900), TaSi$_2$ (1800), ZrSi$_2$, WSi$_2$ (1500), V$_5$Si$_3$ (2260).
Hydrides	TiH$_2$, ZrH$_2$, NbH$_2$.
Intermetallics	NiAl, FeAl, N$_6$Ge, TiNi, CoTi, CuAl.
Chalcogenides	MoS$_2$, TaSe$_2$, NbS$_2$, WSe$_2$.
Cemented carbides	TiC–Ni, TiC–(Ni, Mo), WC–Co, Cr$_3$C$_2$–(Ni, Mo).
Composites	TiC–TiB$_2$, TiB$_2$–Al$_2$O$_3$, B$_4$C–Al$_2$O$_3$, TiN–Al$_2$O$_3$, MoSi$_2$ + Al$_2$O$_3$ (3300), MoB + Al$_2$O$_3$ (4000), Cr$_2$C$_3$ + Al$_2$O$_3$ (6500), 6VN + 5Al$_2$O$_3$ (4800), TiC + Al$_2$O$_3$ (2300).

heat liberated during the reaction is

$$\Delta H^0 = \Delta H^0_{f,298} + \int_{298}^{T_{ad}} \Delta C_p(\text{product}) \, dT$$

where $\Delta H^0_{f,298}$ is the standard enthalpy of formation of the product at 298 K, ΔC_p is the change in heat capacity for the formation of the product.

For a thermally isolated (adiabatic) system, $\Delta H^0 = 0$. Hence

$$-\Delta H^0_{f,298} = \int_{298}^{T_{ad}} \Delta C_p(\text{product}) \, dT \qquad (1)$$

This is shown in Fig. 1. For the case where T_{ad} is less than the melting point, T_{mp}, of the product. If, on the other hand, $T_{ad} = T_{mp}$, then

$$-\Delta H^0_{f,298} = \int_{298}^{T_{ad}} \Delta C_p(\text{product}) \, dT + v\Delta H_m \qquad (2)$$

where v is the fraction of the product that is in the liquid state, and ΔH_m is the heat of fusion of the product. Finally, when $T_{ad} > T_{mp}$, the corresponding relationship will be

$$-\Delta H^0_{f,298} = \int_{298}^{T_{mp}} \Delta C_p(\text{product, solid}) \, dT + \Delta H_m$$
$$+ \int_{T_{mp}}^{T_{ad}} \Delta C_p(\text{product, liquid}) \, dT \qquad (3)$$

In some weakly exothermic reactions ignition can occur only when the reactants are at an elevated (ignition) temperature, T_{ig}. Pre-heating is then needed. Also, the adiabatic temperature is strongly dependent on the ignition temperature, T_{ig} [8]. In this case, the adiabatic temperature can be calculated using one of the following three equations.

$$-\Delta H^0_{f,T_{ig}} = \int_{T_{ig}}^{T_{ad}} \Delta C_p(\text{product}) \, dT \qquad (T_{ad} < T_{mp})$$
$$(4)$$

$$-\Delta H^0_{f,T_{ig}} = \int_{T_{ig}}^{T_{mp}} \Delta C_p(\text{product}) \, dT + v\Delta H_m$$
$$(T_{ad} = T_{mp}) \qquad (5)$$

$$-\Delta H^0_{f,T_{ig}} = \int_{T_{ig}}^{T_{mp}} \Delta C_p(\text{product}) \, dT + \Delta H_m$$
$$+ \int_{T_{mp}}^{T_{ad}} \Delta C_p(\text{product, liquid}) \, dT \qquad (6)$$
$$(T_{ad} > T_{mp})$$

For most compounds the required thermodynamic data can be obtained from data books [9] and, on using the above equations, it is possible to calculate the adiabatic temperature for the reactions. In general, agreement between the experimentally observed combustion temperature, T_c, and the calculated T_{ad} is lacking. This is due to many simplifying assumptions incorporated into the theoretical model. The T_{ad} values calculated using the above equations are essentially upper limits. Nevertheless, the theoretical T_{ad} may be used as a semi-quantitative evaluation. Merzhanov [10] suggested that the system will not become self-sustaining unless $T_{ad} > 1800$ K. Munir [11] found that for material combinations where $T_{ad} < T_{mp}$, the plot of the $\Delta H^0_{f,298}/\Delta C_{p_{298}}$ ratio against T_{ad} has a linear relationship as shown in Fig. 2. From Fig. 2 it can be seen that, for combinations where $\Delta H^0_{f,298}/\Delta C_{p_{298}} \leqslant 2000$ K, a self-propagating mode (i.e. T_{ad} 1800 K) will not be achieved unless some
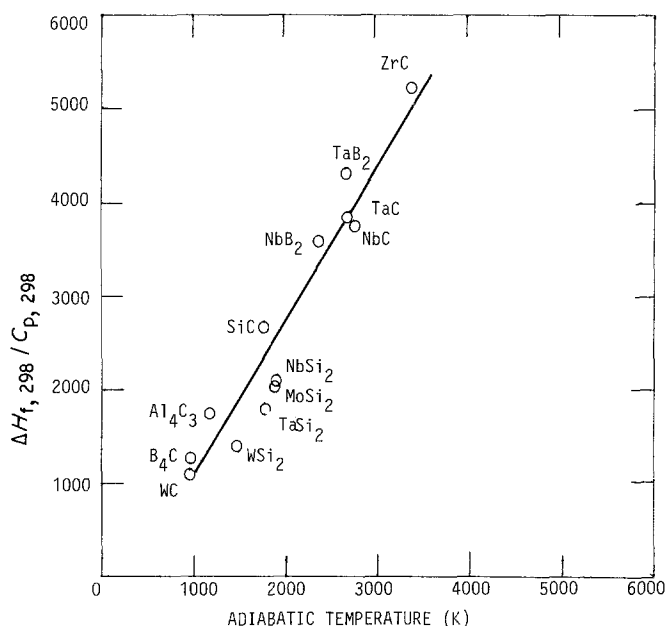
Figure 2 Ratio of the heat of formation of the product to its heat capacity at 298 K plotted against adiabatic temperature (for materials $T_{ad} < T_{mp}$).

external heat source is applied. This could be achieved by either preheating the reactants or by putting them inside another highly exothermic reactant mixture; the latter is termed a "chemical oven".

2.2. The combustion reaction
2.2.1. Stable and unstable combustion
Various combustion phenomena have been observed. Fig. 3 shows photographs of such combustion variations which were obtained by rapid photography techniques used during the combustion process. In most cases steady-state or stable combustion was found for the solid–solid reactions in which the combustion front moves at a constant rate with time (Fig. 3a). Usually, for steady-state combustion, both the reactants and products are in the solid state, i.e. the combustion temperature is less than the lowest eutectic temperature on the phase diagram for the binary reactants. Stable combustion may be converted to an unstable mode on changing the conditions, such as the addition of an inert component or diluent. The propagation of the combustion wave changes with time, as shown in Figs 3b and c which provide examples of two types of unstable combustion, i.e. spinning and auto-oscillating. For the spin combustion, the ignition occurs at a spot on the side of the specimen, and subsequently moves in a spiral path along the side surface of the unreacted section, leaving behind a bright trace which gradually merges with a similar trace from the previous turn. This combustion effects only a narrow surface layer of approximately 2 mm, while the bulk of the sample remains unreacted during the passage of the reaction wave front [12]. However, recent observations of this mode of combustion have shown that combustion can take place throughout the whole sample [13].

During auto-oscillating combustion, periodic oscillations of the combustion front and combustion rate are produced spontaneously, i.e. the wave moves in a succession of fast and slow movements with the instantaneous rate of movement close to a certain mean value. The final product has a layered structure [14]. These layers can be easily divided into discs, with

diameters equal to that of the sample. It has been found that the rate of frequency of the oscillations are affected by the degree of dilution of the initial mixture by inert additions, and the density and diameter of the sample [1].

Fig. 3d shows a photograph of a repeated combustion. It was found that burning hafnium in a nitrogen–argon atmosphere, another wave spontaneously appeared in about 4 sec after passage of the first front but exhibiting a lower rate of motion. It was thought [1] that this repeated combustion was caused by incomplete conversion of the reagents by the first combustion. Thus, the reaction is completed after the second wave passes through.

More complex combustion has been observed for synthesizing nitrides. On igniting powder pellets in a nitrogen atmosphere, two combustion waves were found to be present. These were observed to move towards each other and collide (Fig. 3e). At the collision site a secondary combustion front appeared and moved along the already reacted product at a different rate [15].

2.2.2. Thermal explosion
The thermal explosion technique is achieved on heating a compressed powder compact in a furnace until the combustion reaction occurs simultaneously through the whole sample. This combustion mode is usually used to synthesize intermetallic compounds, because such materials normally need a lower ignition temperature and exhibit lower exothermic heats of reaction. The combustion temperature usually does not exceed 2000° C. Fig. 4 shows a typical exothermic peak which is associated with the combustion reaction. In a study of Ni–Al intermetallic compounds [16], slower heating rates produced two exothermic peaks in some systems. These corresponded to different compound formations. Heating rate, particle size, green density of the pellet have all been found to influence the combustion reaction.

An alternative approach used to react such mixtures would be to utilize the chemical oven technique [11]. For example, the formation of B_4C from a mixture of
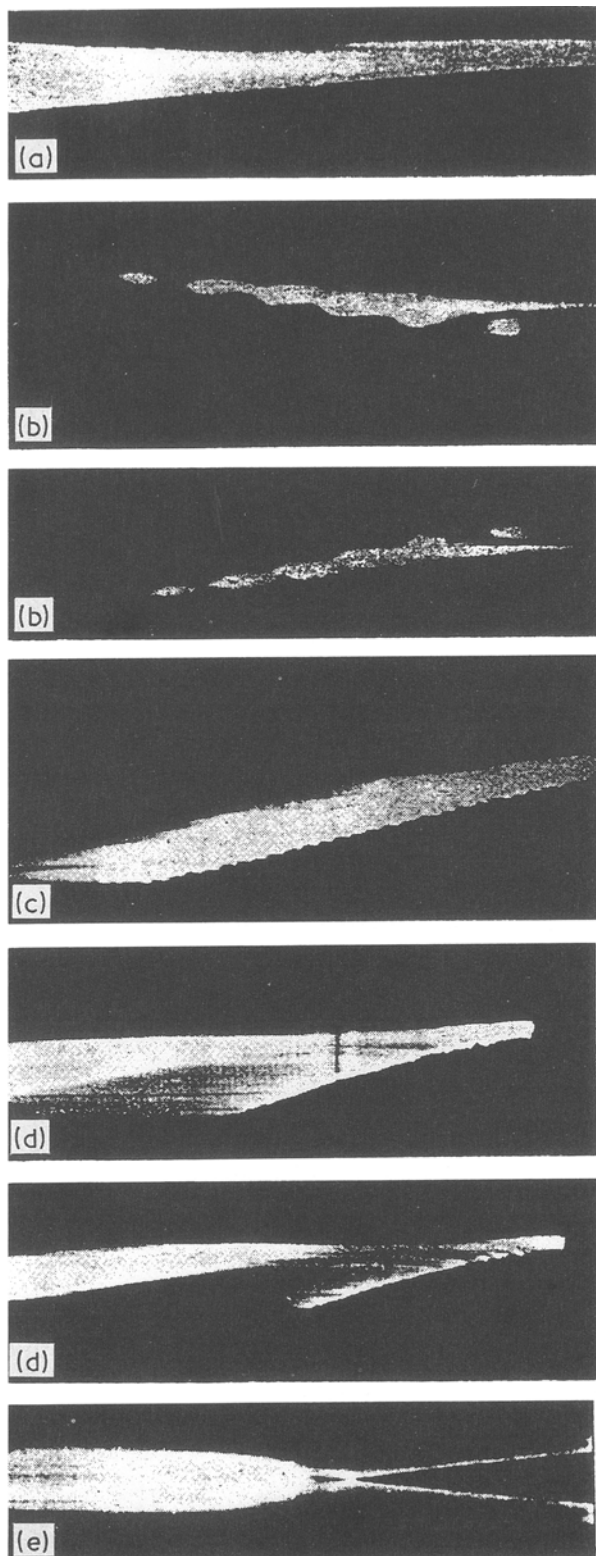
Figure 3 Photographic recording of various types of combustion: (a) stationary combustion; (b) spinning combustion; (c) auto-oscillating combustion; (d) repeated combustion; (e) collision of fronts.

Figure 4 Typical exothermic peak in a thermal explosion mode of combustion.

boron and carbon is a weak exothermic reaction which produces an adiabatic temperature of approximately 1000 K (see Fig. 2). The boron and carbon compact can then be ignited by placing it inside a mixture of titanium and boron (the adiabatic temperature for TiB_2 is 3190 K) and initiating the latter reaction through the standard combustion synthesis method.

2.2.3. Factors influencing the combustion

Fig. 5 shows the dependence of the combustion wave propagation rate and combustion temperature, on various parameters. For Ni–Al intermetallic compounds, it was found that the combustion rate reached a maximum with an equiatomic composition (Fig. 5a) [17]. The combustion temperature also exhibited this trend [8, 16]. With reactant mixtures around the NiAl compound stoichiometry, the combustion mode was one of steady state while for mixtures of Ni_3Al or $NiAl_3$ the combustion mode was pulsating or no reaction at all. This means that in the latter stoichiometric compositions, i.e. $NiAl_3$, the reaction is only weakly exothermic so that both the combustion rate and combustion temperature decrease.

Fig. 5b shows the combustion rate and T_c achieved for different initial preheating temperatures. The higher the pre-heating temperature, the higher the combustion velocity and T_c. This has been found to be the case for both NiAl [8] and CuAl [18] compounds.

Particle size is another factor which influences the combustion because the kinetics of solid state reactions are dependent on the dispersion and the effective contact area of the reactants, as shown in Fig. 5c. It has been found that particle size not only influences the reaction rate, but also the nature of the products formed [11]. In a study of the synthesis of titanium silicide, increasing the titanium particle size from less than $100\,\mu m$ to larger than $100\,\mu m$, the product changed from Ti_5Si_3 to $TiSi_2$ plus titanium [19, 20]. Also, an increase in the titanium particle size changed the mode of combustion from one of steady-state combustion to an unstable spin mode [21]. Using the thermal explosion technique to synthesize NiAl compounds [16], an increase in the particle size has been found to decrease the ignition temperature. The grain size of the reacted product has also been found to be affected by particle size. However, the full influence of particle size on the combustion synthesis reaction is not, as yet, fully understood.

Previously reacted products can be added as a diluent to the unreacted powder mixtures in order to slow down the reaction (Fig. 5d). The amount of
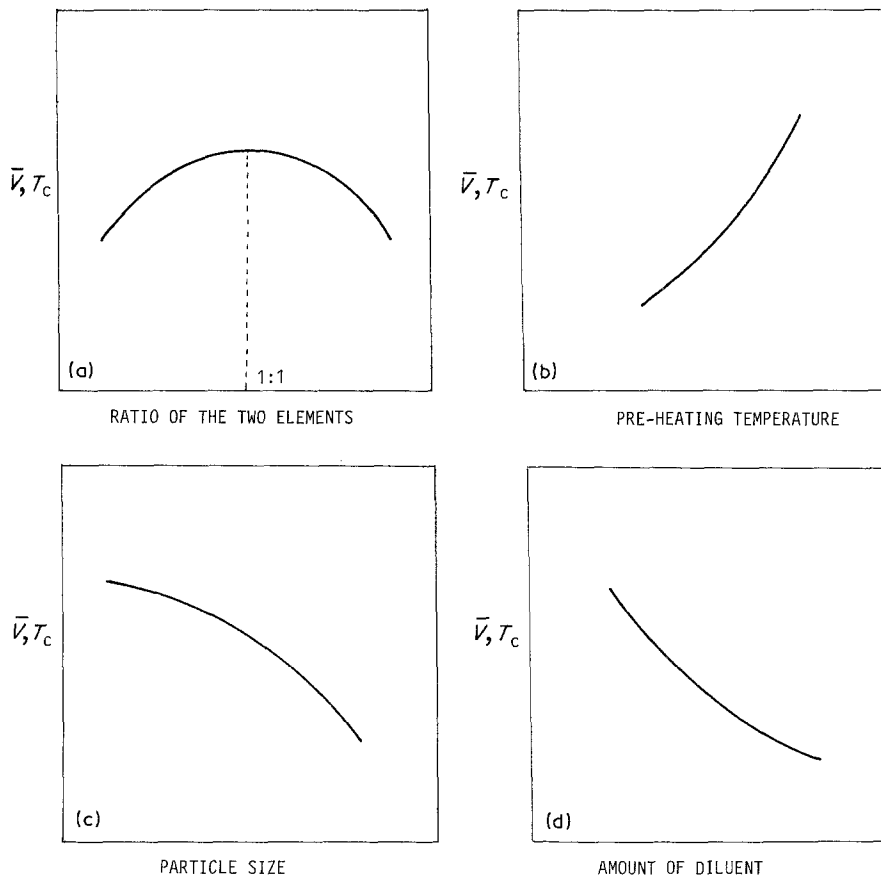
Figure 5 Effect of (a) stoichiometry, (b) pre-heating temperature, (c) particle size, and (d) amount of diluent on propagation rate ($\bar{V}$) and combustion temperature (T_c).

diluent can be as high as 60%. Holt and Munir [7] found that the addition of 10% TiC to a mixture of Ti + C caused a decrease in combustion temperature from 2720 to 2518 K.

2.3. Combustion theory

2.3.1. Combustion propagation velocity

As the products are formed during the combustion reaction, two important factors, i.e. the velocity of the propagation wave ($\bar{V}$) and the combustion temperature (T_c), need to be determined. This can be achieved from both theoretical (mathematical) and empirical methods. The fundamental mathematical considerations were developed in the 1950s [22, 23]. Fig. 6 is a schematic representation of the temperature and velocity profile of the propagation wave where it can be seen that both the combustion and temperature profiles move with the same velocity. At any point in the sample a heat balance equation can be given by [24]

$$C_p\varrho\,\frac{dT}{dt} = k\nabla^2 T + \varrho Q W(\eta, T) - q(T - T_0)$$

$$- \frac{2\varepsilon\sigma_0}{r}(T^4 - T_0^4) \tag{7}$$

[conduction] + [chemical reaction]

− [convection] − [radiation]

where C_p is the heat capacity (J g^{-1} K^{-1}), ϱ the density of the pellets (g cm^{-3}), T the temperature (K), t the time (sec), k the thermal conductivity (W cm^{-1} K^{-1}), x, y, z, coordinates (m), Q the heat of reaction (J g^{-1}), $W(\eta, T)$ the reaction rate, η the reacted fraction, q the heat loss coefficient (W cm^{-3} K^{-1}), r the sample

radius (cm), ε the emissivity coefficient, σ_0 the Stefan–Boltzman constant (W cm^{-2} K^{-4}), T_0 the ambient temperature (K), and

$$\nabla^2 T = \frac{d^2 T}{dx^2} + \frac{d^2 T}{dy^2} + \frac{d^2 T}{dz^2}$$

The four terms on the right-hand side of Equation 7 represent heat generated by conduction and chemical reaction and heat lost by convection and radiation, respectively. The function, $W(\eta, T)$, can usually be represented in the following form

$$W(\eta, T) = \frac{d\eta}{dT} = \bar{V}_a\nabla\eta$$

$$= (1 - \eta)^n K_0 \exp(-E/RT) \tag{8}$$

where $\bar{V}_a$ is the adiabatic combustion wave velocity, E the activation energy, R, universal gas constant, n, K_0 are the order of the reaction and the pre-exponential constant, respectively, and $\nabla\eta = d\eta/dx$ (one
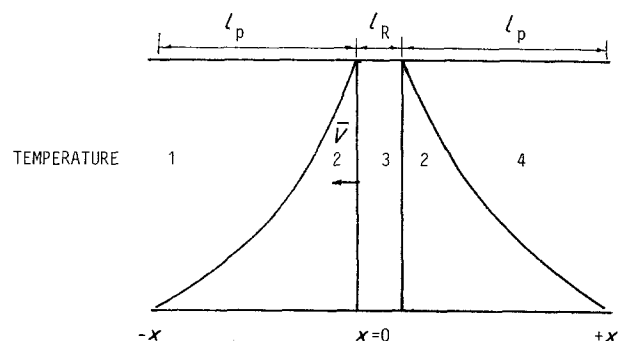
Figure 6 Representation of the propagating wave velocity and the temperature profile during the combustion synthesis reaction. 1, Reactants; 2, temperature profile; 3, reaction zone; 4, product.
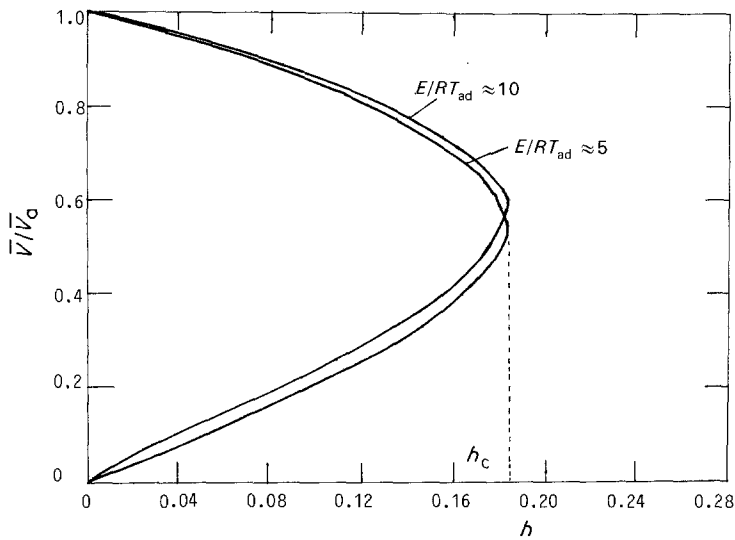
dimensional). In general, to a first approximation, the convective and radiative heat losses may be omitted so that Equation 7 becomes

$$C_p \varrho \frac{dT}{dt} = kV^2 T + \varrho Q(1 - \eta)^n K_0 \exp(-E/RT)$$
(9)

Fig. 6 shows the reaction propagation front in which there is a reaction zone, of width l_R, and a preheat zone, of width l_p. The widths of these two zones are related by [25]

$$l_R = \frac{l_p RT_{ad}}{E}$$
(10)

where T_{ad} is the adiabatic temperature (theoretical value of the combustion temperature). For reactions with very large activation energies, the width of the reaction zone is narrow compared with that of the heating zone

i.e. $$\frac{E}{RT_{ad}} \gg 1$$

$$l_R \ll l_p$$
(11)

Based on this condition, and an added stipulation that the heat flow between the reactant and product can be neglected, using appropriate boundary conditions, an explicit expression of adiabatic velocity, $\bar{V}_a$ has been derived for steady-state combustion [26, 27]

$$\bar{V}_a^2 = f(n) \frac{aC_p(T_{ad})^2}{QE} K_0 \exp(-E/RT_{ad})$$
(12)

where a is the thermal diffusivity and $f(n)$ is a complicated constant function, the value of which depends on the order of reaction, n.

According to Equation 12, Holt *et al.* [28] measured the activation energy for the combustion of the Ti + 2B = TiB$_2$ system using different amounts of TiB$_2$ product as a diluent in the reactant mixture in order to vary the combustion velocity and temperature. Because the activation energy of conventionally sintered TiB$_2$ was found to be larger than that of the combustion synthesis reaction for TiB$_2$, they concluded that the two types of reaction do not occur by the same mechanism.

When $T_{ad} > T_{mp}$ a liquid phase is expected. Margolis [29] presented a model allowing for such melting of the product. For $n = 1$ in Equation 9, he derived a multi-term expansion for the steady, planar, adiabatic reaction speed. The first term is:

$$\bar{V}_a^2 = \frac{aC_p R(T_{ad})^2}{QE} K_0 \exp[-E/RT_{ad}]$$

$$\times \left\{ \frac{\alpha}{1 + (\gamma/Q)} - \left[\frac{\alpha}{1 + (\gamma/Q)} - 1 \right] \right.$$

$$\left. \times \exp\left[\frac{E}{R(T_{ad})^2} (T_{mp} - T_{ad}) \right] \right\}$$
(13)

where α is a constant representing that the reaction-rate jumps by a factor α when melting occurs due to the increased surface-to-surface contact of the reactants, γ is the heat of fusion. In the limit of $\alpha \to 1$, $\gamma \to 0$, i.e. no melting occurs or melting has no effect on the propagation of the reaction front, Equation 13 becomes exactly the same as Equation 12.

It should be pointed out that the above consideration is based on homogeneous, adiabatic combustion. If the heat loss term in Equation 7 is neglected: i.e. $q \neq 0$, the combustion becomes non-adiabatic. An analytical calculation for this case was conducted recently [30] in which the homogeneous non-adiabatic combustion velocity, V, was

$$V/\bar{V}_a = 1/a_0[a_0^2 - h/\Delta]$$
(14)

where h is a heat loss parameter (proportional to the heat loss coefficient q) and $\Delta \simeq E/RT_{ad} \gg 1$; a_0 is a constant, the value of which depends on h and the melting parameter M (see Equation 16), $\bar{V}_a$ is the adiabatic combustion velocity as shown in Equation 13. Fig. 7 shows the relationship between $V/\bar{V}_a$ and the heat loss parameter h at $T_{ad} < T_m$. It can be seen that no solution exists for Equation 14 when $h > h_c$. h_c is an extinction limit beyond which no steady burning can occur, although unstable combustion may still exist beyond this limit. On the other hand, only the upper part of the curve in Fig. 7, which contains the adiabatic solution $\bar{V} = \bar{V}_a$, is stable. The stable non-adiabatic velocity decreases with increase in heat losses.

2.3.2. Steady-pulsating transitions

As stated in Section 2.2.1, the combustion may be changed from stable to unstable when some parameters change. There have been a number of theoretical attempts to explain this phenomenon. First a numerical solution was used to calculate Equation 9 in which n was equal to unity [31]. The result showed that there are two qualitatively different reaction front propagation regimes: steady-state and oscillatory. In the first regime, as soon as the combustion is established, both the temperature profile and the amount reacted advance through the sample at a constant rate equal to the burning rate, V. During the oscillatory regime, the combustion velocity oscillates about the steady-state value, but the mean velocity of the pulsations is less than that of the uniformly propagating state, with the difference increasing as the activation energy increases [32]. In particular, as pointed out by Matkowsky and Sirashinsky [33], uniform propagation occurs when the activation energy (E) is smaller than that which applies to unstable (oscillatory) propagation. Based on the numerical result, a parameter, α, was proposed to be the neutral boundary between stable and unstable combustion:

$$\alpha = \frac{RT_{ad}}{E}\left[9.1\,\frac{C_p T_{ad}}{Q} - 2.5\right] \quad (15)$$

If $\alpha > \alpha_c = 1$, steady-state combustion is stable, but if $\alpha < \alpha_c$, combustion proceeds in an oscillatory mode. In other words, Equation 15 shows that the activation energy in stable combustion is less than that in pulsating combustion.

The first analytical calculation for Equation 9 $(n = 1)$ was accomplished by Matkowsky and Sivashinsky [33]. They have shown that a solution exhibiting a periodically pulsating reaction front arises as a Hopf bifurcation from a solution representing a uniformly propagating front. The bifurcation parameter is

$$\alpha = \frac{EQ}{2RC_p(T_{ad})^2} \quad (16)$$

with the critical value $\alpha_c = 2 + 5^{1/2}$. If $\alpha > \alpha_c$ the combustion will be unstable in a pulsating mode. In particular, they have also shown analytically that the

velocity of the oscillatory front is indeed less than that of the steady propagating plane front.

It is interesting to compare the above theoretical results with experimental data. Table II lists the maximum activation energy for a steady-state combustion to occur for those materials in which their adiabatic temperatures are less than their melting points. In the calculations, the value of $Q/C_p = \Delta H_{f,298}/C_{p,298}$ was used. From Table II it can be seen that both models do not satisfy Equation 11 very well although the second model is much better than the first. Fig. 8 shows the neutral boundary between stable and pulsating combustion where it is seen that a roughly linear relationship between E and T_{ad} exists. For the materials with lower activation energy, the steady-state combustion is actually impossible, and for those materials (e.g. left corner of Fig. 8), no combustion occurs due to the lower exothermic behaviour, and the reaction cannot become self-sustaining.

In general, the theoretically calculated values of E are less than the experimentally derived data. For example, for ZrC, $E = 170.8\,\text{kJ}\,\text{mol}^{-1}$ [34], but both theoretical values are less than this (Table II). Also for TiC, the actual activation energy is much larger than theoretical prediction [7]. Although this indicates that improvements in the theoretical calculations should be considered, the model by Matkowsky and Sivashinsky [33] is much better than that of Shkadinskii *et al.* [31].

Margolis [29] investigated the effect of melting on the bifurcation phenomenon. The bifurcation parameter was found to be

$$\alpha = \frac{EQ}{2C_p R(T_{ad})^2(1 - M)} \quad (17)$$

where M is the melting parameter $0 < M < 1$. The non-melting case corresponds to $M = 0$. The critical bifurcation parameter, α_c, is still equal to $2 + 5^{1/2}$. The effect of melting is to make the pulsating regime more feasible and instability can occur for reactions with lower activation energies as shown in Fig. 9. This means that the bigger the value of M, the more liquid will result and the combustion will tend to be unstable. Thus from this conclusion the combustion synthesis of TiNi, ZrN and NbN should be more unstable because their adiabatic temperatures are much larger than

TABLE II Upper activation energy values for the stable combustion of selected products from their elements; calculation from Equations 14 and 15 ($T_{ad} < T_{mp}$)

Materials	T_{mp} (K)	T_{ad} (K)	$\Delta H_{f,298}/C_{p,298}$ (K)	E (kJ mol^{-1})		E/RT_{ad}	
				[14]	[15]	[14]	[15]
WC	3058	1000	1 132	62.2	46.1	7.5	5.5
B$_4$C	2743	1000	1 363	51.7	34.7	6.2	4.2
Al$_4$C$_3$	2500	1200	1 786	56.7	36	5.7	3.6
WSi$_2$	2433	1500	1 443	109.8	86.6	8.8	7.0
TaSi$_2$	2473	1800	1 823	125.2	97.1	8.4	6.5
SiC	3259	1800	2 714	84.1	52.9	5.6	3.5
MoSi$_2$	2302	1900	2 058	123.6	93.2	7.8	5.9
NbSi$_2$		1900	2 137	119	88.3	7.5	5.6
NbB$_2$	3273	2390	3 643	110.5	69.0	5.6	3.5
TaC	4273	2700	3 891	132.0	85.6	5.9	3.8
TaB$_2$	3373	2700	4 348	118.1	70.7	5.3	3.2
NbC	3500–3753	2800	3 781	146.1	98.7	6.3	4.2
ZrC	3805	3400	5 241	155.4	96.2	5.5	3.4

Thermodynamic data are from [9].
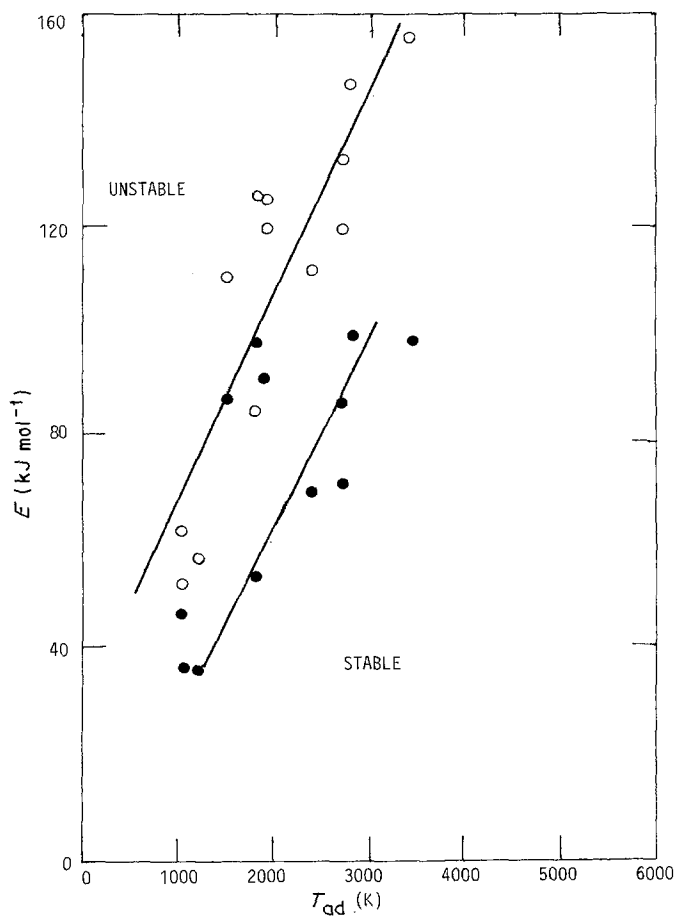
Figure 8 Relationship between activation energy, E, for stable and unstable combustion and adiabatic temperature, T_{ad}, indicating the neutral boundary between stable and unstable combustion: (○) from Equation 15, (●) from Equation 14.

their melting points. It should be mentioned here that the above considerations apply only to homogeneous combustion. For the heterogeneous case, the reader should consult works by Margolis and co-workers [30, 35].

3. Combustion synthesis of intermetallic compounds

Numerous intermetallics have been produced using the SHS method. Of these, aluminides have received considerable attention, in particular aluminides with nickel [8, 16, 36–40], copper [18, 41, 42] and zirconium [43]. Other intermetallics include titanium with cobalt and iron [44] and nickel shape-memory alloys [45–47]. In the preparation of aluminides either the combustion or thermal explosion modes can be used. It has been demonstrated that the products of reactions are the same irrespective of the experimental technique used. For the combustion mode, both the combustion rate and temperature are greatly affected by the preheating of the reactants. For example, in the NiAl system [8] the combustion temperature increased from 1900 K to nearly 2100 K on increasing the preheating temperature to 500° C. In the latter case, the product was initially in the liquid state. As for the thermal explosion mode, heating rate plays an important role. The combustion temperature can be greatly increased on using a higher heating rate. More important, it was found that the microstructure of the product changed with different heating rates [16]. The higher the heating rate, the denser the product. This latter observation was believed to be due to the higher heating rates providing a lower probability of forming pre-combustion (diffusional) phases which have the ability

to make the product more porous [11]. The addition of small amounts of boron (0.5 at %) to the Al + Ni reactant mixture resulted in an even lower level of porosity. However, it is still not quite clear what role the boron plays in the mechanism of combustion synthesis of nickel aluminides.

Recently, shape-memory alloys (SMA) have received considerable research attention. This type of alloy changes its shape due to crystallographic changes associated with variations in temperature with corresponding changes in properties which create considerable potential usage in both military and commercial applications. Of many such alloys, intermetallic nickel–titanium has been given more attention. Conventionally, the alloy is produced by arc or induction melting with the cast alloy usually displaying some degree of segregation. This conventionally produced TiNi SMA is difficult to machine. In contrast, powder metallurgy techniques can produce alloys with minimum segregation. Some Soviet researchers have synthesized this type of alloy using the combustion mode of the SHS method. However, the product had a high degree of porosity [48, 49]. The authors are also currently engaged in a research programme using the thermal explosion mode of SHS for producing this alloy [50, 51]. A fully densified cast alloy has been obtained.

4. Combustion synthesis of refractory nitrides

Nitrides possess important properties such as high refractoriness, hardness and chemical stability which makes these materials widely applicable. For example, TiN, ZrN and HfN can be used as grinding tools, catalysts for heterogeneous gas–solid reactions and
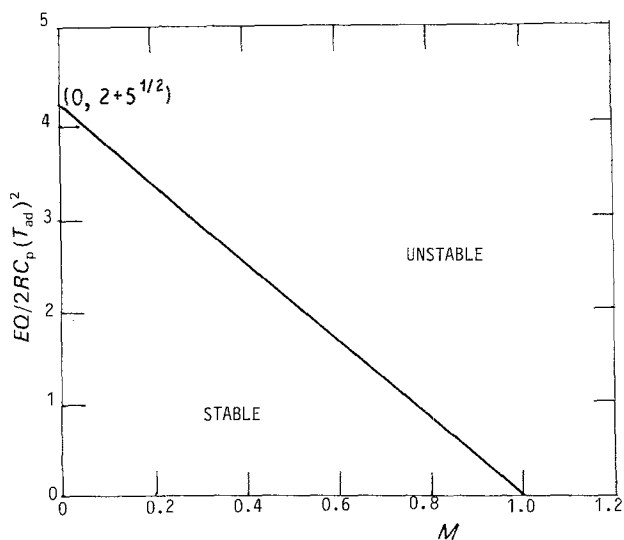
Figure 9 Effect of melting on the neutral stability boundary, after [29].

crucibles for containing molten metal, respectively. Silicon nitride is used in microelectronic devices because of its chemical stability. A variety of nitride phases has been prepared using either gaseous or liquid nitrogen [1, 52–55] in the combustion synthesis mode.

At first it was found that when combustion was carried out at 1 atm pressure of nitrogen, the nitride product was in a low degree of conversion (< 50%). This was because of the relatively high combustion temperature (> 2500° C) produced during the reaction creating a molten phase which formed a kinetic barrier for any further reaction to proceed. As mentioned earlier, one solution to the problem is to add the product phase as a diluent in order to lower the combustion temperature. However, this method still does not obtain 100% conversion. Complete conversion of titanium to titanium nitride has been found possible if a significant fraction of nitride phase is added as a diluent together with the application of a high nitrogen pressure (~ 10 MPa) [55]. Another way to overcome this difficulty is to add nitrogen in a solid form, e.g. sodium azide (NaN_3) [52], which decomposes at low temperature. Metal powders (e.g. titanium, zirconium, hafnium, yttrium) compacted with NaN_3 in stoichiometric proportions have produced 100% conversions. Scanning electron microscopy (SEM) and emission spectrochemical analysis indicated that the products were of high purity with the sodium completely volatilized and removed. This process has also been used to produce composite ceramic materials, e.g.

$$3TiO_2 + 4Al + NaN_3 = 3TiN + 2Al_2O_3 + Na_{(g)}$$
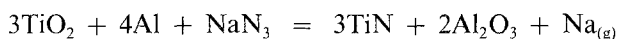
It should be pointed out that as the nitrides have a high dissociation pressure, a high pressure of nitrogen gas has to be used. The pressure must equal or exceed the dissociation pressure of the nitride at the combustion temperature [52, 53]. Si_3N_4, AlN, BN, Cubic TaN and β' SIALON have been produced by this method.

5. Densification method

Typically, SHS produced materials are very porous

(about 50% dense). Porosity is caused by outgassing of the absorbed gases and voids existing in the compacted pellets. Hence the products are primarily used in powder form after grinding. Recently, research has been conducted to obtain a densified product in a single operation.

Holt [52, 56] used simultaneous synthesis and application of force to obtain high-density materials with a variety of techniques. For example, pressure (2000 to 4000 psi, 13.8 to 27.6 N mm^{-2}) was applied to the product by uniaxial pressing a few seconds after the combustion temperature reached its maximum. The method has successfully produced 95% dense TiC and 98% dense TiB_2. Other techniques including explosive compaction, isostatic pressing and the application of shock waves generated in a gas gun, have also been used with the Ti + 2B reaction. Explosively compacted TiB_2 was found to be somewhat porous, but both isostatic pressing and the use of a gas gun produced TiB_2 with densities greater than 90% theoretical.

Another way to densify the products is to use a liquid phase in the combustion process. Theoretically, the adiabatic temperature must be higher than the melting point of the product so that a cast alloy can be obtained. A number of composite ceramics have been synthesized using this method, but, as mentioned in Section 2.3.2 this can lead to unstable combustion.

6. Conclusions

The major advantages of the SHS technique are concerned with improvements in process energy and time, simplicity of the SHS processing technique and the potential for producing high-purity products possessing a high degree of metastability. The latter point also indicates the potential for producing new materials with unique properties. The ability to produce composite ceramic materials from cheaper raw materials, such as oxides reacted with carbon or other elements will also provide considerable incentives for increasing the research effort in this technique.

Almost all of the known ceramic materials can be produced using the SHS method, including [11]:

1. abrasives, cutting tools, polishing powders, e.g. TiC cemented carbides and carbonitrides;

2. elements for resistance heating furnaces, e.g. $MoSi_2$;

3. high-temperature lubricants, e.g. chalcogenides of molybdenum;

4. neutron attenuators, e.g. refractory metal hydrides;

5. shape-memory alloys, e.g. TiNi;

6. high-temperature structural alloys, e.g. Ni–Al;

7. steel melting additives, e.g. nitrided ferro alloys;

8. electrodes for electrolysis of corrosive media, e.g. TiN.

The major disadvantages are concerned with achieving high product density and tight control over the reaction and products.

Considerable further research is needed in order to: more fully understand the influence of processing parameters on product properties; provide simultaneous synthesis and densification of the product; explore the

range of materials that can be produced from this technique; investigate the problems associated with scale-up and production of finished or near net-shape products.

References

1. A. G. MERSHANOV and I. P. BOROVINSKAYA, *Comb. Sci. Tech.* **10** (1975) 195.
2. L. M. SHEPPARD, *Adv. Mater. Proc.* February **2** (1986) 25.
3. B. MANLEY, J. B. HOLT and Z. A. MUNIR, *Mater. Sci. Res.* **16** (1984) 303.
4. O. R. BERMANN and J. BARRINGTON, *J. Amer. Ceram. Soc.* **49** (1966) 502.
5. M. OUABDESSELAM and Z. A. MUNIR, *J. Mater. Sci.* **22** (1987) 1799.
6. D. R. GASKELL, "Introduction to Metallurgical Thermodynamics" (McGraw-Hill, New York, 1973) p. 26.
7. J. B. HOLT and Z. A. MUNIR, *J. Mater. Sci.* **21** (1986) 251.
8. V. M. MASLOV, I. P. BOROVINSKAYA and A. G. MERZHANOV, *Comb. Explos. Shock Waves* **12** (1976) 631.
9. I. BARIN, K. KNACKE and O. KUBACHEWSKI, "Thermochemical properties of inorganic substances" (Suppl.) (1977).
10. A. G. MERZHANOV, in "Combustion Processes in Chemical Technology and Metallurgy", edited by A. G. Merzhanov (Chernogolovka, 1975).
11. Z. A. MUNIR, *Ceram. Bull.* **67** (1988) 342.
12. A. K. FILONENKO and V. I. VERSHINNIKOV, *Comb. Explos. Shock Wave* **11** (1975) 301.
13. Y. M. MAKSIMOV, A. G. PAK, G. V. LAVRENCHUK and Y. S. NAIBORODENKO, *ibid.* **15** (1979) 415.
14. I. P. BOROVINSKAYA, A. G. MERZHANOV, N. P. NOVIKOV and A. K. FILONENKO, *ibid.* **10** (1974) 2.
15. A. G. MERZHANOV, A. K. FILONENKO and I. P. BOROVINSKAYA, *Dokl. Akad. Nauk SSSR (Phys. Chem.)* **208** (1973) 122.
16. K. A. PHILPOT, Z. A. MUNIR and J. B. HOLT, *J. Mater. Sci.* **22** (1987) 159.
17. Y. S. NAIBORODENKO and V. I. ITIN, *Comb. Explos. Shock Wave* **11** (1975) 626.
18. V. I. ITIN, A. D. BRATCHIKOV and A. V. LEPINSKIKH, *ibid.* **17** (1981) 506.
19. N. P. NOVIKOV, I. P. BOROVINSKAYA and A. G. MERZHANOV, in "Combustion Processes in Chemical Technology and Metallurgy", edited by A. G. Merzhanov (Chernogolovka, 1975).
20. A. R. SARKISYAN, V. K. DOMBROVSKA, I. P. BOROVINSKAYA and A. G. MERZHANOV, *Comb. Explos. Shock Wave* **14** (1978) 310.
21. T. S. AZATYAN, V. M. MELTSEV, A. G. MERZHANOV and V. A. SELEZNEV, *ibid.* **15** (1979) 35.
22. F. BOOTH, *Trans. Faraday Soc.* **49** (1953) 272.
23. R. A. W. HILL, *Proc. Roy. Soc. London* **226A** (1954) 455.
24. A. G. STRUNINA, T. M. MARTEMYANOVA, V. V. BARZYKIN and V. I. ERMAKOV, *Comb. Explos. Shock Wave* **10** (1974) 449.
25. W. B. BUSH and F. E. FENDELL, *Comb. Sci. Tech.* **1** (1970) 421.
26. B. I. KHACHIN and A. G. MERZHANOV, *Comb. Explos. Shock Wave* **2** (1966) 22.
27. B. V. NOVOSHILOV, *Dokl. Akad. Nauk SSSR* **144** (1962) 1328.
28. J. B. HOLT, B. D. KINGMAN and G. M. BIANCHINI, *Mater. Sci. Engng* **71** (1985) 321.
29. S. B. MARGOLIS, *SIAM J. Appl. Math.* **43** (1983) 351.
30. H. G. KAPER, G. K. LEAF, S. B. MARGOLIS and B. J. MATKOWSKY, *Comb. Sci. Tech.* **53** (1987) 289.
31. K. G. SHKADINSKII, B. I. KHAIKIN and A. G. MERZHANOV, *Comb. Explos. Shock Wave* **7** (1971) 15.
32. Y. B. ZELDOVICH, O. I. LEGPUNSKY and J. B. LIBROVICH, "Theory of Non-steady powder combustion" (Izdat. Nauka, Moscow, 1975).
33. B. J. MATKOWSKY and G. I. SIVASHINSKY, *SIAM J. Appl. Math.* **35** (1978) 465.
34. A. P. HARDT and P. V. PHUNG, *Comb. Flame* **21** (1973) 77.
35. S. B. MARGOLIS, *Comb. Sci. Tech.* **43** (1985) 197.
36. Y. S. NAIBORODENKO and V. I. ITIN, *Comb. Explos. Shock Wave* **11** (1975) 293, 626.
37. A. P. HARDT and R. W. HOLSINGER, *Comb. Flame* **21** (1973) 91.
38. Y. S. NAIBORODENKO, V. I. ITIN and K. V. SAVITSKII, *Sov. Phys. J.* **11** (1968) 19, 89.
39. Y. S. NAIBORODENKO, V. I. ITIN, A. G. MERZHANOV, I. P. BOROVINSKAYA, V. P. USHAKOV and V. P. MASLOV, *ibid.* **16** (1973) 872.
40. Y. S. NAIBORODENKO, V. I. ITIN, B. P. BELOZEROV and V. P. USHAKOV, *ibid.* **16** (1973) 1507.
41. Y. S. NAIBORODENKO, V. I. ITIN and K. V. SAVITSKII, *Sov. Powd. Metall. Met. Ceram.* **7** (91) (1970) 562.
42. V. I. ITIN, A. D. BRATCHIKOV and L. N. POSTNIKOVA, *ibid.* **5** (209) (1980) 315.
43. E. A. NEKRASOV, V. M. MAKSIMOV and A. P. ALDUSHIN, *Comb. Explos. Shock Wave* **17** (1981) 140.
44. V. I. ITIN, A. D. BRATCHIKOV, A. G. MERZHANOV and V. M. MASLOV, *ibid.* **17** (1981) 293.
45. V. I. ITIN, V. N. KHACHIN, A. D. BRATCHIKOV, V. E. GYUNTER, E. F. DUDAREV, T. V. MONASEVICH, D. B. CHERNOV, G. D. TIMONIN and A. P. PAPERSKI, *Sov. Phys. J* **20** (1977) 1631.
46. A. D. BRATCHIKOV, A. G. MERZHANOV, V. I. ITIN, V. N. KHACHIN, E. F. DUDAREV, V. E. GYUNTER, V. M. MASLOV and D. B. CHERNOV, *Sov. Powd. Metall. Met. Ceram.* **1** (205) (1980) 5.
47. V. I. ITIN, Y. S. NAIBORODENKO, A. D. BRATCHIKOV, N. P. BUTKEVICH, S. V. KOROSTELEV and L. V. SHOLOKHOVA, *Sov. Phys. J.* **18** (1976) 408.
48. V. I. ITIN, V. N. KHACHIN, V. E. GYUNTER, A. D. BRATCHIKOV and D. B. CHERNOV, *Sov. Powd. Metall. Met. Ceram.* **5** (243) (1983) 156.
49. V. I. ITIN, A. D. BRATCHIKOV, V. N. DORONIN and G. A. PRIBYTKOV, *Sov. Phys. J.* **24** (1981) 1134.
50. H. C. YI and J. J. MOORE, *J. Mater. Sci.* **24** (1989) 3455.
51. *Idem, ibid.* **24** (1989) 3462.
52. J. B. HOLT, Lawrence Livermore National Laboratories, LLL-TB-84, May (1986).
53. Z. A. MUNIR and J. B. HOLT, *J. Mater. Sci.* **22** (1987) 710.
54. J. B. HOLT and Z. A. MUNIR, in Proceedings of the First International Symposium on Ceramic Components for Engine, edited by S. Somiya, E. Karnai and K. Ando, Hakone, Japan (1984) p. 721.
55. K. HIRAO, Y. MIYAMOTO and M. KOIZUMI, *Materials (Jpn)* **36** (400) (1987) 12.
56. J. B. HOLT, *Mater. Bull.* October–November (1987) 60.